Journal of Hydrology: Regional Studies 45 (2023) 101306

Contents lists available at ScienceDirect

Journal of Hydrology: Regional Studies

journal homepage: www.elsevier.com/locate/ejrh

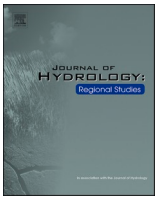

Watershed model parameter estimation in low data environments

Roja K. Garna [a,d], Daniel R. Fuka [a], Joshua W. Faulkner [b], Amy S. Collick [c], Zachary M. Easton [a,*]

[a] Department of Biological Systems Engineering, Virginia Tech, Blacksburg, VA, USA
[b] Department of Plant and Soil Science, University of Vermont, Burlington, VT, USA
[c] Department of Agricultural Sciences, Morehead State University, Morehead, KY, USA
[d] Stantec Consulting Services Inc., Lexington, KY, USA

ARTICLE INFO

Keywords:
Calibration
Low data environments
Regionalization
SWAT model

ABSTRACT

Study region: Three watersheds in the Lake Champlain Basin of Vermont, USA.
Study focus: Watershed models are essential for evaluating the impact of watershed management; however, they contain many parameters that are not directly measurable. These parameters are commonly estimated by calibration against observed data, often streamflow. Unfortunately, many areas lack long-term streamflow records, making parameter estimation in low data environments (LDE) challenging. A new calibration technique, simultaneous multi-basin calibration (MBC), was developed to estimate model parameters in LDE. Three Soil and Water Assessment Tool (SWAT) model initializations for USGS gages with ~ 2-year records in the Lake Champlain Basin of Vermont, USA, were evaluated by comparing MBC and the commonly used similarity-based regionalization (SBR) approach, where calibrated parameters from a watershed with an extended data record are transferred to the LDE receptor watersheds. In MBC, each watershed is initialized, and observed flows from each initialization are aggregated to generate a combined streamflow record of sufficient length to calibrate using a differential evolution algorithm.
New hydrological insights for the region: Using this new MBC method, we demonstrate improved model performance and more realistic model parameter values. This study demonstrates that short periods of hydrological measurement from multiple locations in a basin can represent a system similarly to long term measurements and that even short records taken at multiple locations significantly improve our hydrologic knowledge of a system as compared to relying on the similarity of a basin with a long record of flow. In addition, this study revealed that the hydrologic response is mediated by the interplay of very low soil-saturated hydraulic conductivity (Ksat) and cracking soils. As a result, even if Ksat is very low, cracking clays have a large impact on runoff production Garna et al. (2022).

1. Introduction

Watershed scale hydrological models are often used to quantify and predict diverse and complicated hydrologic system behavior and are often used to manage environmental and water resources. A process based hydrological model consists of equations and parameters that describe watershed processes such as snow accumulation, groundwater flow, runoff generation, and

* Correspondence to: Virginia Tech, 303 Seitz Hall, 155 Ag Quad Lane, Blacksburg, VA 24061, USA.
E-mail address: zeaston@vt.edu (Z.M. Easton).

https://doi.org/10.1016/j.ejrh.2022.101306
Received 10 June 2022; Received in revised form 9 December 2022; Accepted 12 December 2022
Available online 15 December 2022
2214-5818/© 2022 The Authors. Published by Elsevier B.V. This is an open access article under the CC BY license (http://creativecommons.org/licenses/by/4.0/).

evapotranspiration (Devia et al., 2015; Sorooshian et al., 2008). Since hydrological models represent simplified versions of natural processes, they are inherently uncertain (Moges et al., 2020; Orth et al., 2015; Renard et al., 2010; Wagena et al., 2019). The primary sources of uncertainty are model structure (simplified process representation), input data (limited measurements), and parameter estimation (difficulties in specifying exact parameter values) (Ehlers et al., 2018; Gupta and Govindaraju, 2019; Jin et al., 2010; Moges et al., 2020; Setegn et al., 2009). Many parameters in watershed-scale models cannot be measured directly due to process complexity, limitations in measurement methods, and spatiotemporal heterogeneity. Therefore, it is necessary to estimate the parameter value through model calibration (Gupta and Govindaraju, 2019). Model calibration adjusts the model parameters within feasible parameter ranges (Veith et al., 2010) so that model responses, such as streamflow, show good agreement with the observed values (Singh and Frevert, 2002). Hydrologic systems are characterized by complex processes and many interactions, and are driven by exogenous forcing, making model parameter estimation critical and often difficult. This is especially apparent in watersheds without long-term data, or in regions characterized by rapid environmental change (Mirza, 2011; Schiermeier, 2011; Trenberth, 2009, 2005; Wagena et al., 2016).

In addition, insufficient information about model parameter values makes it difficult to model hydrological systems in their full complexity and heterogeneity. Natural variability is thus aggregated to a great extent by models leading to the potential of equifinality, the situation when there is more than one possible model parameter set that results in suitable simulation results (Beven, 1993; Seibert et al., 2019). Equifinality is intensified by over-parameterization (Her and Chaubey, 2015), and is one of the most common issues that hydrologists encounter while using hydrological models (van Griensven et al., 2006). Therefore, it is necessary to constrain the calibration processes to only those most influential parameters using sensitivity analysis (Veith et al., 2010).

Streamflow is one of the primary observed measurements used to calibrate watershed models because it is a good integrator of the hydrological mass balance for a basin, and various processes occurring in the watershed such as atmospheric exchange, soil moisture redistribution, runoff generation, and evapotranspiration (Hui et al., 2020; Wambura et al., 2018). Successful calibration often requires a suitable record of observed streamflow (Daggupati et al., 2015). However, in many watersheds, observed streamflow data are unavailable or only exist for short durations (Sivapalan et al., 2003), making calibration a challenging process.

To deal with this problem and to estimate streamflow in low data environments (LDE), two different regionalization techniques are commonly used (Blöschl and Sivapalan, 1995): statistically-based (Sivapalan et al., 2003; Yadav et al., 2007) and similarity-based (Farsadnia et al., 2014; Mengistu et al., 2019; Rafiei Emam et al., 2017; Vandewiele and Elias, 1995). Statistical-based approaches identify relationships between calibrated model parameters in watersheds with adequate available data and watershed attributes in LDE, such as soil type, topography, or drainage area (Lee et al., 2006; Parajka et al., 2005). Previous studies often report statistical methods unable to suitably simulate streamflow (Merz and Blöschl, 2004; Peel et al., 2000). The similarity-based approach (Similarity Based Regionalization-SBR) estimates LDE watershed model parameters by transferring parameter values from a "donor", often nearby, watershed with a suitable calibration (Masih et al., 2010; Samuel et al., 2011; Vandewiele and Elias, 1995). While SBR is the most commonly used techniques for parameter estimation in LDE, it is challenging to obtain representative parameter estimates (Sivapalan et al., 2003), because the uncertainty embedded in the parameters of the donor watershed directly impact (and often increase) the uncertainty of parameters in the LDE (Sellami et al., 2014). Comparisons of the statistically based and regionalization methods show that the regionalization methods result in better model simulations, with studies from Bao et al. (2012), Merz et al. (2011), and Oudin et al. (2008) investigating 55 watersheds in China, 308 watersheds in Australia, and 913 watersheds in France, respectively, all showing better performance of SBR under multiple-hydroclimate conditions.

This study demonstrates a new simultaneous multi-basin calibration (MBC) method that can be used to calibrate basins with short streamflow records in LDE. To test the new method, we use three newly instrumented United States Department of Agriculture (USDA)-Natural Resources Conservation Service (NRCS) Conservation Effects Assessment Project (CEAP) watersheds (USDA NRCS, 2019) with short streamflow duration records ($\sim$ 2 years) and a donor watershed with 31 years of daily streamflow data. We select twelve years of streamflow data of the donor watershed from 2010 to the present because more than 10-years of recorded streamflow data is a common length for calibration, and needed to adequately represent hydroclimatic variability (Feyereisen et al., 2007; Oeurng et al., 2011; Shi et al., 2011). The three newly instrumented watersheds are located at distances 1, 23, and 25 km from the watershed with a longer record, distances often cited as appropriate for parameter regionalization (Lebecherel et al., 2016). The results of the new MBC methodology are compared to the SBR regionalization technique of using a neighboring basin with a longer streamflow duration record (donor watershed), and by comparing calibrated parameters and simulated streamflow obtained by the SBR and MBC in the three low-data watersheds. To demonstrate the extent to which the methods capture physical processes within the basin, we compare calibrated parameters against measured soil data collected in the watersheds, including soil depth, saturated hydraulic conductivity, and available water capacity (all calibrated parameters in the model as well). The objective of this work is to develop a new calibration method that improves model performance and increases the information content of watershed models in Low Data Environments and to improve model parameter estimation to enhance process understanding.

2. Materials and methods

2.1. Study area

The study area is located within the Lake Champlain Basin (LCB) of Vermont (VT), USA. Lake Champlain is a 193-kilometer-long freshwater lake on the western border of VT that provides drinking water to approximately 200,000 people in the US and Québec. The lake is a large economic generator for the region (approx. $3.8 billion generated over 1998–1999 (LCBP, 2016)). Lake Champlain has been subject to periodic harmful algal blooms (HABs), which most commonly occur in a number of shallow bays spread throughout the

Vermont shoreline. Elevated phosphorus (P) delivery to freshwater systems has been documented to contribute to HAB formation (Davis et al., 2010; Huang et al., 2020), and is generally considered a key factor driving occurrence in Lake Champlain. Dairy farming is the primary agricultural sector in the VT portion of the basin, and approximately 38 % of the total P reaching the lake is estimated to be from nonpoint agricultural sources (Troy et al., 2007). The Little Otter Creek (LOCB) and the Dead Creek (DCB) basins are both located in the southern portion of the basin, within 10 km of one another and have recently (2019) been instrumented as USDA-NRCS CEAP watersheds to quantify the environmental effects of conservation practices and programs to guide USDA conservation policy and program development under agreements between USGS and USDA. The LOCB with an area of 158 square kilometers (km^2) above the USGS gage "04282650" (LOC-Ferrisburg) (U.S. Geological Survey, 2021a) and the DCB with an area of 96 km^2 above the intersection of Vermont Route 17 (VT 17) and Dead Creek are located in Addison County, Vermont, within the Champlain Valley physiographic province (Stewart and Macclintock, 1969), which drain into Lake Champlain at Hawkins Bay and Fields Bay, respectively (Fig. 1). Weather data from closest Global Historical Climate Network (GHCN) weather stations (Menne et al., 2012, Fig. 1) show that precipitation in the area averages 1058 millimeters per year. The mean annual maximum temperature is 13.2 °C, while the mean minimum temperature is 1.9 °C. The physiography of DCB watersheds are relatively uniform, with a mean slope of 2.7°, and a maximum of 53.4°. The LOCB watersheds have a mean of 5.7° and maximum of 57.9° (Fig. 1). The soil data obtained from the USDA's WebSoilSurvey (Web Soil Survey, 2019) show that the area is dominated by Vergennes clay (2–6 % slope (40 %), 6–12 % slope (7.2 %), and 12–25 % slope (16.3 %)), Covington and Panton silty clays (21 %), and silt loams (11 %) (Fig. 1). The minimum and maximum elevation of the study area are 45 m and 185 m, respectively.

Fifty soil samples were collected across LOCB and DCB watersheds from the depth of 6 in. in the fall of 2020 by the Vermont Association of Conservative Districts (USDA NRCS, 2019). These soil samples were analyzed using the Cornell Soil Health protocol (Moebius-Clune et al., 2016) for soil texture and available water capacity (AWC). Soil depth and saturated hydraulic conductivity (Ksat) were estimated based upon field measurements using a constant head permeameter and observations within the watershed area. The region is also characterized by swelling-cracking clay soils with very low Ksat < 1 mm/h in many areas (Ruggiero et al., 2022).

The watersheds, LOC-Ferrisburg and "USGS 04282629 - Little Otter Creek-Monkton" (LOC-Monkton) (U.S. Geological Survey, 2021b) are located in LOCB and "USGS 04282586 - West Branch Dead Creek" (WBDC) (U.S. Geological Survey, 2021c), and "USGS 04282581 - East Branch Dead Creek" (EBDC) (U.S. Geological Survey, 2021d) located in DCB were calibrated using daily streamflow records from the U.S. Geological Survey (USGS) gaging stations (U.S. Geological Survey, 2022). LOC-Monkton, WBDC, and EBDC are three newly instrumented watersheds with short measured streamflow data from September 2019 to November 2021 (26 months) that were considered as receptor watersheds in the SBR calibration method. LOC-Ferrisburg with a longer streamflow record (31-years daily streamflow) was the donor watershed in SBR methodology.

The primary land cover classes within all watersheds are pasture/hay (43 %), forest (21 %), and row crop agriculture (5 %), based on an analysis from the Multi-Resolution Land Characteristics (MRLC) national land cover (NLCD 2016) dataset (Dewitz, 2021).

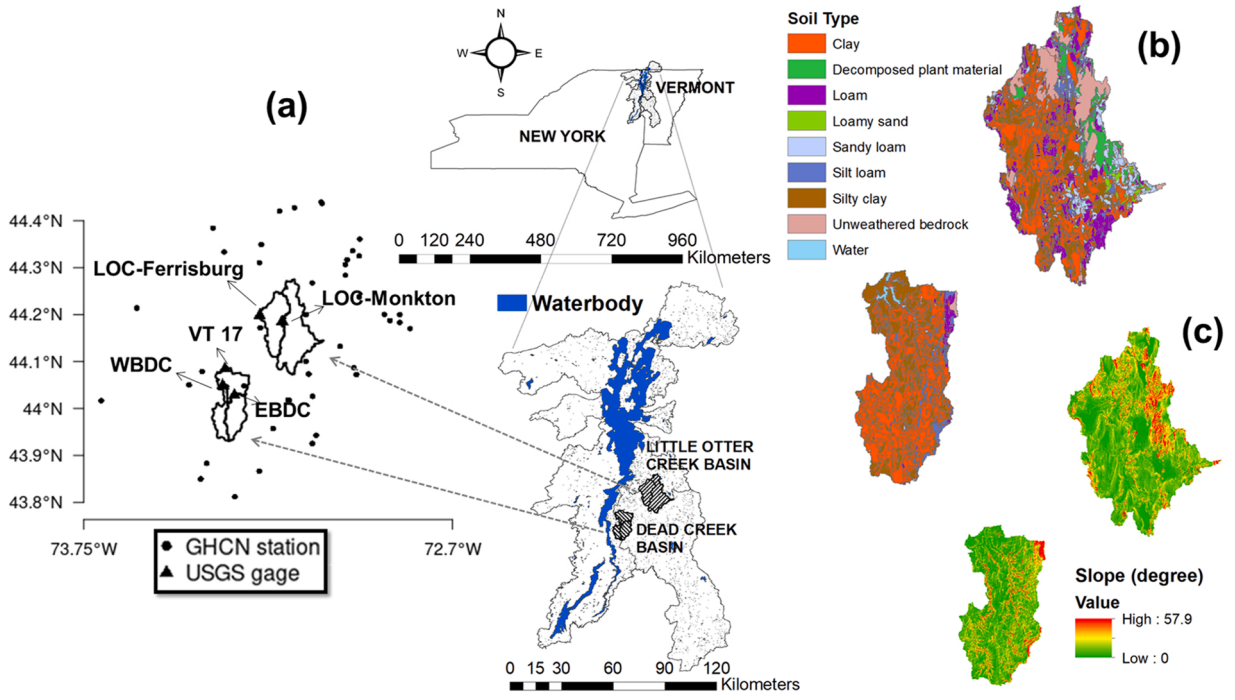

Fig. 1. The location (a), soil map (b), and slope map (c) of the study area. The map shows the locations of watersheds, GHCN weather stations, and stream gauging stations.

2.2. Hydrologic model initialization

The Soil and Water Assessment Tool (SWAT), a semi-distributed process-based watershed-scale hydrologic model developed by the USDA (Arnold et al., 1998), was selected because it has been widely used for watershed assessment and management with over 5000 peer-reviewed articles (Gassman et al., 2014, 2010). SWAT simulates the land phase and routing phase of the hydrologic cycle to predict the impact of different management actions on crop production and environmental quality modeled using representations of the watershed, divided first into sub-basins, then each sub-basin divided into Hydrologic Response Units (HRUs) based on similar landcover, soil type, slope class, and management (Arnold et al., 2013).

For this study, we used an adaptation of the SWAT model (rev 681) in the R modeling language, the SWATmodel package (Fuka et al., 2014b), which provides a linear-model-like R interface to the SWAT modeling system, including an optimization process using the DEoptim R Package (Ardia, 2009; Fuka et al., 2014a, 2012; Collick et al., 2015; Esmali et al., 2020), an R based function with simple objective function creation around a differential evolution algorithm (a type of genetic algorithms that uses the operations of crossover, mutation, and selection on population with successive generations) for global optimization; especially useful in hydrological modeling where the objective function is noisy, and difficult to differentiate (Mullen et al., 2011). DEoptim was used to perform both sensitivity analysis and calibration processes. To handle the uncertainties in input parameters, the parameter ranges were selected and constrained based on prior knowledge about the study area (see Table 1). We used the "build_swat_basic()" function in SWATmodel to extract a simplified three basins, 9 HRUs, quasi-lumped model of the watershed above the USGS gages. The basic data required to run SWATmodel are the USGS gage information (including the size of drainage area, elevation of the gage, latitude, and longitude of the gage) and meteorological forcing data. The meteorological data, including daily precipitation, minimum and maximum temperature were obtained automatically by the "FillMissWX()" function from the R EcoHydRology package, which uses the Inverse Distance Weighting (IDW) method (Hubbard, 1994) to estimate missing data from the GHCN weather stations within 30 km of the USGS gages. Fig. 1 shows all the GHCN stations within 30 km of the outlet of the watersheds; together, these comprise the allowable stations from which weather data are obtained.

For the SBR donor watershed, LOC-Ferrisburg, was initialized identically to the other basins, though the IDW weather assimilation was completed for both the seven years (2015–2021) period, and the more common calibration duration of twelve years (2010–2021).

Table 1
SWAT parameters, their definitions, typical range, and modification type considered for the **sensitivity** analysis and their sensitivity ranks.

Parameter	Definition	Range	Modification	Process	Level
ALPHA_BF	Baseflow alpha factor (days)	0–1	Replacement of the value	Groundwater	HRU
SMFMX	Melt factor for snow on June 21 (mm/°C/day)	0–5	Replacement of the value	Snow	Subbasin
CN2	SCS runoff curve number for moisture condition II	45–90	Replacement of the value	Runoff	HRU
Ksat (%)	Soil saturated hydraulic conductivity (mm/h)	0.3–3	Multiplier	Soil	HRU
TIMP	Snowpack temperature lag factor	0.01–1	Replacement of the value	Snow	Subbasin
Depth (%)	Soil depth	0.3–3	Multiplier	Soil	HRU
GW_DELAY	Groundwater delay (days)	0–1000	Replacement of the value	Groundwater	HRU
AWC (%)	Available water capacity (mm/mm soil)	0.3–3	Multiplier	Soil	HRU
ESCO (in HRU files)	Soil evaporation compensation factor	0.1–1	Replacement of the value	ET	HRU
SURLAG	Surface runoff lag coefficient	0–15	Replacement of the value	Runoff	Subbasin
RCHRG_DP	Groundwater recharge to deep aquifer (fract)	0–1	Replacement of the value	Groundwater	HRU
GWQMN	Threshold depth of water in the shallow aquifer required for return flow to occur (mm)	0–600	Replacement of the value	Groundwater/ Soil	HRU
EPCO (in HRU files)	Plant uptake compensation factor	0.1–1	Replacement of the value	ET	HRU
SMFMN	Melt factor for snow on December 21 (mm/°C/day)	0–5	Replacement of the value	Snow	Subbasin
SMTMP	Snow melt base temperature (°C)	-5 to 5	Replacement of the value	Snow	Subbasin
SFTMP	Snowfall temperature (°C)	-5 to 5	Replacement of the value	Snow	Subbasin
GW_REVAP	Groundwater “revap” coefficient	0–0.3	Replacement of the value	Groundwater	HRU
REVAPMN	Threshold depth of water in the shallow aquifer for “revap” to occur (mm)	0–500	Replacement of the value	Groundwater	HRU

2.3. Sensitivity analysis

To constrain the calibration to only those parameters most influential, a sensitivity analysis was conducted (Saltelli, 2004; Vemuri et al., 1969). Based on a review of published SWAT literature, 18 parameters that affect modeled flow were selected for sensitivity analysis (Table 1) (Cibin et al., 2010; Khorashadi Zadeh et al., 2017; Leta et al., 2015; Nossent and Bauwens, 2012).

To conduct the sensitivity analysis, we used "DEoptim()" function within the R DEoptim package to generate five datasets of 300 evolutionary optimization iteration parameter (Table 1) sets aligned with the progressively increasing Nash-Sutcliffe model efficiency coefficients (NSEs) for each of the periods 2015–2021 and 2010–2021 (10 datasets in total). Each output is therefore a 300 $\times$ 19 data frame, the first 18 columns of which are the SWATmodel parameter values (Table 1), and the last column is the NSE value between simulated and observed streamflow at LOC-Ferrisburg for that parameter set. In the optimization, the NSE was used as the objective function, the number of attempts between evolutions of the parameter vector (NP) was set to 16. In the next step, a 299 $\times$ 19 data frame was generated using the changes of individual steps for the optimized parameter values and the corresponding NSE between two successive iterations. Considering the amount of change in each parameter and the NSE, we removed the parameter that resulted in no change in the NSE on any of the 300 successive iterations. The remaining parameters are sensitive or influential parameters, and therefore retained for calibration (Table 1).

2.4. Similarity based regionalization (SBR)

Similarity based regionalization (SBR) model calibration is based on the assumption of similarity between the donor (LOC-Ferrisburg) and receptor (LOC-Monkton, WBDC, and EBDC) watersheds. Attributes most often used to asses suitability of donor and receptor watersheds in the SBR calibration approaches include watershed drainage area, landcover, slope, soil type, mean annual precipitation, maximum and minimum temperature, elevation, and proximity (Tegegne and Kim, 2018). As shown in Section 2.1, all watersheds have approximately similar physical characteristics. Weather data for all four watersheds showed adequate similarity based on Pearson correlation coefficients (r) for precipitation and maximum and minimum temperature ($r > 0.99$), and average absolute error for average temperature and precipitation (0.11 mm for precipitation and 0.20 °C for temperature) as suggested by Deshmukh et al. (2022).

Model calibration was performed on the sensitivity index determined parameters in Table 1 for the LOC-Ferrisburg donor watershed using the DEoptim package for 2010–2021 and 2015–2021. The optimized parameter set from calibration was then transferred to three neighboring receptor watersheds (LOC-Monkton, EBDC, and WBDC). Model performance was assessed using the NSE (a good statistic for peak flow evaluation), ratio of the root mean square error to the standard deviation of measured data (RSR) (a

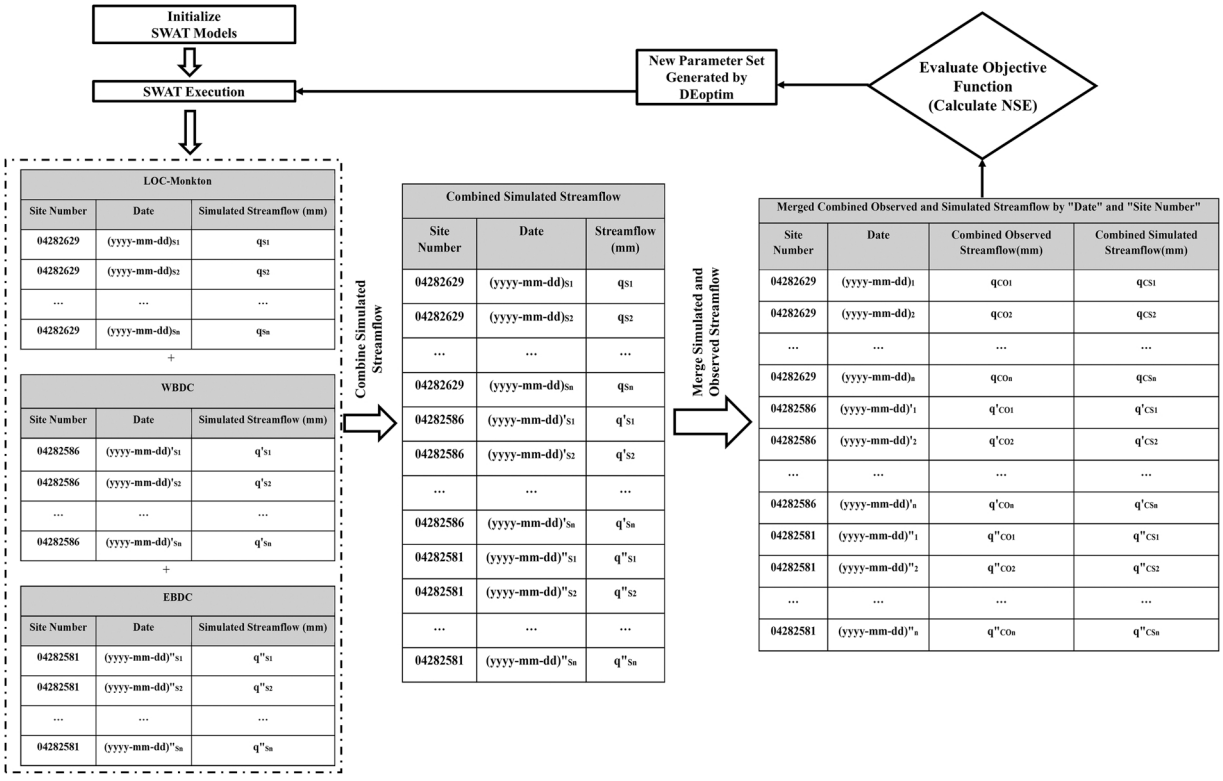

Fig. 2. Schematic of the simultaneous multi-basin calibration method (MBC).

good indicator for average flow conditions), and percent bias (PBIAS), an indicator of over/under prediction of simulated flows, for each watershed, as recommended by Moriasi et al. (2007).

2.5. Simultaneous calibration of multiple watershed models (MBC)

The multi basin calibration (MBC) approach consists of two primary steps; first, streamflow data from each of three LDE watersheds (LOC-Monkton, EBDC, and WBDC) are aggregated, and second, these data are then calibrated as a single dataset. Fig. 2 shows the MBC method framework. Observed streamflow data, obtained from the USGS gages discussed previously, are aggregated to create a data frame of combined observed streamflow. The combined observed streamflow data frame includes the individual site number, the date, and streamflow (mm) for each watershed. Therefore, instead of having only 2-yrs of observed data to calibrate the model the combined observed streamflow data frame now contains 6 years of observed of daily streamflow data (3 watersheds * 2-yrs data each). This serves to increase the information content, improving both the estimates of model parameters and the simulated streamflow. After creating combined the observed streamflow data frame, SWAT models of each LDE watershed are initialized individually, then, the modeled streamflow is generated by execution of the models with an initial (default) parameter set with default values from the input data. Following model execution, the simulated streamflow (mm), date, and corresponding site number from each modeled watershed are aggregated (as described above) to build a combined simulated, although uncalibrated, streamflow data frame (Fig. 2). Then, the combined observed and simulated streamflow data frames are merged by "Date" and "Site Number" resulting in a new data frame with the observed and simulated flow for the three watersheds merged by date and site number (merged combined observed and simulated streamflow data frame in Fig. 2). This data frame is the one that is subjected to calibration (Fig. 2). Over each iteration of the calibration a new parameter set is generated by the DEoptim algorithm is used by SWAT for the model execution step, finally, the NSE is evaluated (Fig. 2). The calibration process will stop when the maximum number of iterations is reached. The simulated streamflow using MBC was assessed for the goodness of fit against observations using NSE, RSR, and PBIAS for each watershed, as recommended by Moriasi et al. (2007).

2.6. Model evaluation and corroboration

Due to the short period of recorded streamflow data in each of the watersheds (~ 2 yrs) and because hydrological simulations are often subject to non-stationary conditions, the use of the typical split-sampling approach does not capture the variability in the watershed, and using full-time series calibration is more robust (Singh and Bárdossy, 2012; Arsenault et al., 2018). Therefore, we calibrated the model for daily streamflow simulation for the entire ~6 yr time series. To evaluate the model performance, we used bootstrapping resampling to obtain the probability distribution of the performance indicators (NSE, RSR, and PBIAS) over the entire available ~ 6 yr time period (Efron, 1992; Canty, 2002). The bootstrap test was performed using 1000 samples of observed and simulated streamflow datasets from each of the SBR and MBC methods for each watershed.

We also evaluated several model parameters against measurements made in the watersheds and against estimates from the Soil Survey Geographic (SSURGO) database from Natural Resources Conservation Service (NRCS) (http://websoilsurvey.sc.egov.usda.gov-(Web Soil Survey, 2019)) using the "soilDB" package in R (Beaudette et al., 2021). Among all the parameters listed in Table 1, soil Ksat, soil AWC, and soil depth were collected from 50 locations across LOCB and DCB, and compared to model estimated values.

In addition to streamflow, the SWAT model also estimates the major water balance components, including evapotranspiration (ET), surface flow, lateral flow, groundwater flow, and percolation. Following model calibration, the average annual water balance components of three watersheds obtained from each calibration method were assessed.

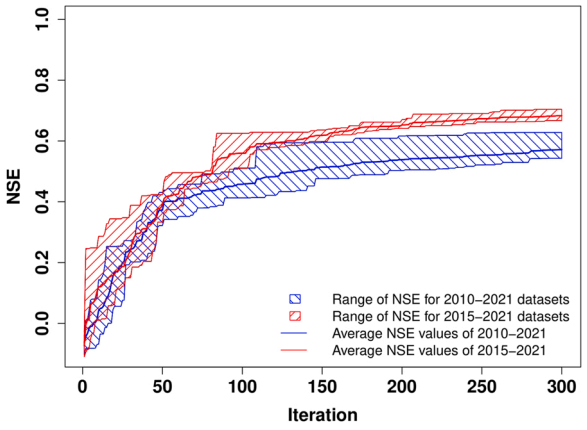

Fig. 3. NSE values of 10 datasets over 300 iterations. The blue and red shaded zones are the range of NSE values in each iteration for 2010–2021 and 2015–2021, respectively. The blue and red solid lines represent the average of NSE values in each iteration for 2010–2021 and 2015–2021, respectively.

3. Results and discussion

3.1. Sensitivity analysis

Fig. 3 shows the NSE values (solid line shows average, shading shows range) of 10 datasets, consisting of five datasets of 300 iterations for 2015–2021 and five datasets of 300 iterations for 2010–2021 generated by the DEoptim algorithm for each iteration of the optimization. 300 iterations were selected for sensitivity because we have found it to adequately represent moderate dimension problems, and 300 iterations consumed most of the computational time allocated. As seen in Fig. 3, the rate of NSE changes decreases significantly after iteration 200 compared to the first 200 iterations for each dataset, showing that the setting of maximum iteration number to 300 was sufficient for optimization. In addition, the ranges of the maximum NSE values after 300 iterations for 2010–2021 and 2015–2021 are 0.55–0.62 and 0.66–0.70, respectively. The potential reason for the difference between NSE values for these two time periods is that the latter simulates the shorter simulation period with less variability (Mohammed et al., 2021) and that 93 % of the weather data for 2015–2021 are obtained from the closest station.

3.2. Calibration

Among the most sensitive parameters shown in Table 1, the average condition CN2 value was calibrated independently for each HRU based on previous studies in the LCB, which indicated it is characterized by variable source area hydrological response (Buchanan et al., 2018; Twombly et al., 2021). In SWAT the CN2 is adjusted in the HRU management input files (*.mgt). Since we have three HRUs in each subbasin in our study, the CN2 was adjusted in the first (*1.mgt), second (*2.mgt), and third (*3.mgt) HRU management files representing downslope, midslope, and upslope HRUs. For estimation of the range of CN2 in each HRU, an initial estimate of the CN2 for the entire watershed was calculated by the method described in Lyon et al. (2004) as applied by Easton et al. (2011), and was equal to 84. In order to account for the effect of hillslope position and terrain on runoff generation as estimated by the curve number, the CN2 for downslope HRUs (CN2(*1.mgt)), midslope HRUs (CN2(*2.mgt)), and upslope HRUs (CN2(*3.mgt)) calibrated with the range of 65–75, 75–85, and 85–95, respectively so that the area-weighted CN2 equaled 84. Also, the range of AWC (%, multiplier) in Table 1 was 2–2.5 with the initial value of 2.25 to constrain AWC in the same range as measured field AWC.

3.2.1. Calibration of the LOC-Ferrisburg donor watershed for SBR

The LOC-Ferrisburg donor watershed was calibrated to maximize the NSE and minimize the RSR and PBIAS between observed and simulated streamflow on a daily time step for 2010–2021 and 2015–2021. The calibration result showed good agreement between the daily simulated and observed streamflow, with NSE, RSR, and PBIAS of 0.51, 0.69, and − 22, respectively for 2010–2021 and 0.61, 0.60, and − 24, respectively for 2015–2021. The optimized parameters from the calibrated watershed for each period are given in Table 2.

3.2.2. SBR receptor watershed model performance

For the similarity-based approach, the parameter sets (2010–2021 and 2015–2021 calibrated parameters) obtained from the calibration of the LOC-Ferrisburg donor watershed (Table 2) were transferred to three receptor watersheds (LOC-Monkton, WBDC, and EBDC) to simulate daily streamflow. The SBR calibration in LOC-Monkton resulted in moderately well-simulated streamflow (NSE = 0.57 for 2010–2021 & 0.60 for 2015–2021, RSR = 0.65 for 2010–2021 & 0.63 for 2015–2021, PBIAS = − 24 for 2010–2021 &

Table 2
List of the optimized parameter values from calibration results using similarity-based approach (SBR) for 2010–2021 and 2015–2021 and simultaneous calibration of multiple basins (MBC) method. CN2 (*1.mgt), CN2 (*2.mgt) and CN2 (*3.mgt) indicate the curve numbers that assigned to the downslope, midslope and upslope HRUs management input files (*.mgt), respectively.

Parameter	SBR (2010–2021)	SBR (2015–2021)	MBC	Modification
GW_DELAY	6.25	3.35	25.84	Replacement of the value
ALPHA_BF	0.91	0.52	0.94	Replacement of the value
GWQMN	9.31	7.58	188	Replacement of the value
RCHRG_DP	0.33	0.18	0.31	Replacement of the value
SFTMP	1.13	1.20	3.49	Replacement of the value
SMTMP	0.77	0.74	0.52	Replacement of the value
SMFMX	4.10	2.08	4.66	Replacement of the value
SMFMN	2.05	1.21	1.50	Replacement of the value
TIMP	0.66	0.58	0.91	Replacement of the value
SURLAG	0.16	0.22	0.57	Replacement of the value
Depth	1.05	0.90	2.93	Multiplier
AWC	2.22	2.16	2.47	Multiplier
Ksat	2.69	2.47	0.57	Multiplier
ESCO	0.78	0.70	0.68	Replacement of the value
EPCO	0.90	0.90	0.78	Replacement of the value
CN2 (*1.mgt)	65	66	65	Replacement of the value
CN2 (*2.mgt)	84	84	84	Replacement of the value
CN2 (*3.mgt)	94	94	95	Replacement of the value

− 23 for 2015–2021), but did not result in adequate streamflow simulation for WBDC and EBDC and there were some differnces in the water balance as well (Figs. 4, 5). The adequate performance at LOC-Monkton is likely a result of the LOC-Monkton drainage area representing approximately one half of the total area of LOCB. That is, the flows that are generated in LOC_Monkton significantly affect the flows of LOC_Ferrisburg, while flows of WBDC and EBDC are independent of LOC_Ferrisburg (Fig. 1). While LOC_Monkton drains into LOC_Ferrisburg station and in practice, the LOC_Monkton sub-watershed is already calibrated while calibrating the model to the LOC_Ferrisburg's data, this study used the short period LOC_Monkton records as the third LDE to determine the potential benefits of using multiple short records from a region.

3.2.3. Simultaneous calibration of multiple basins -MBC

In this new calibration technique, three watersheds (LOC-Monkton, WBDC, and EBDC) with short durations of measured data were calibrated simultaneously. The optimized parameter set obtained by MBC is listed in Table 2. Then, the parameters obtained from MBC were used to simulate streamflow in individual watersheds. The NSEs between simulated and observed streamflow were 0.52, 0.50, and 0.60 for LOC-Monkton, WBDC, and EBDC watersheds, respectively. The RSR values were 0.68 for LOC-Monkton, 0.69 for WBDC, and 0.63 for EBDC. The PBIAS values were − 25 for LOC-Monkton, 20 for WBDC, and − 1 for EBDC.

3.3. Comparison between SBR and MBC

Considering the widespread use of watershed models to analyze or predict environmental and hydrological processes, calibration of watershed models in LDE is one of the most challenging and fundamental issues in computational hydrology. Regionalization is one of the most common approaches used to calibrate watershed models in LDE. Several studies have shown good performance of regionalization methods (Merz and Blöschl, 2004; Vandewiele and Elias, 1995), but adequate performance is often contingent on the proximity of watersheds with long term, high-quality data. For instance, Randrianasolo et al. (2011) showed that the optimum distance between donor and receptor watersheds is less than 18 km to achieve the highest model performance. Indeed, as indicated by the poor model performance for the WBDC and EBDC watersheds using SBR, where the donor watershed is 23–25 km away, the distance between the donor and receptor watersheds is of considerable importance.

3.3.1. Comparison of parameter estimates and water balance components between SBR and MBC

Several of the parameters listed Table 2 show notable differences between the methods while others are remarkably similar. For instance, Table 2 shows that the CN2 values in the upslope, midslope, and downslope HRUs are similar for all methods, indicating consistency among methods with respect to runoff generation. This is further corroborated by Fig. 4, which shows the contribution of ET, surface runoff, lateral flow, percolation, and baseflow to the overall water balance from each calibration method for the study area. The values of surface runoff were similar among methods, and ranged from 155 mm (MBC) to 165 mm (SBR 2015–2021), about 15 % of the water balance. These are also similar to previous studies in the region, such as Wagena and Easton (2018) who estimated annual average surface runoff of 108 mm (also approximately 15 % of the water balance for the Susquehanna River basin in NY and PA. Easton et al. (2008) also estiamted simialr surface runoff losses of ~150 mm in the Catskill region of NY.

Table 2 also shows that soil Depth (%, multiplier) and AWC (%, multiplier) have greater values for MBC than both SBR realizations, and Ksat (%, multiplier) has a lower value. The greater depth and AWC values for MBC result in greater soil moisture storage, reducing lateral flow and percolation, and making more moisture available for ET, which is also confirmed in the water balance (Fig. 4). The lower Ksat for MBC may also contribute to lower lateral flows and percolation.

The surface runoff lag coefficient (SURLAG) differs substantially between MBC (0.57) and SBR 0.16–0.22), with SURLAG 2–3 times greater using the MBC method (Table 2). SURLAG controls the timing of the surface runoff contribution to the total flow; as SURLAG increases, the surface runoff that is stored in the catchment decrease. Previous studies (TetraTech, 2013) using SWAT in the Lake Champlain Basin estimated SURLAG to be 0.5, similar to the MBC method.

Snow parameters also differed among methods (Table 2), with MBC calibrations resulting in higher snowpack temperature (TIMP), snowfall temperature (SFTMP) and melt factor (SMFMX and SMFMN) parameters, and lower snowmelt base temperature (SMTMP) parameters, all of which leads to less snow accumulation and faster melt rates than in SBR calibrations. As the snow melts faster, more

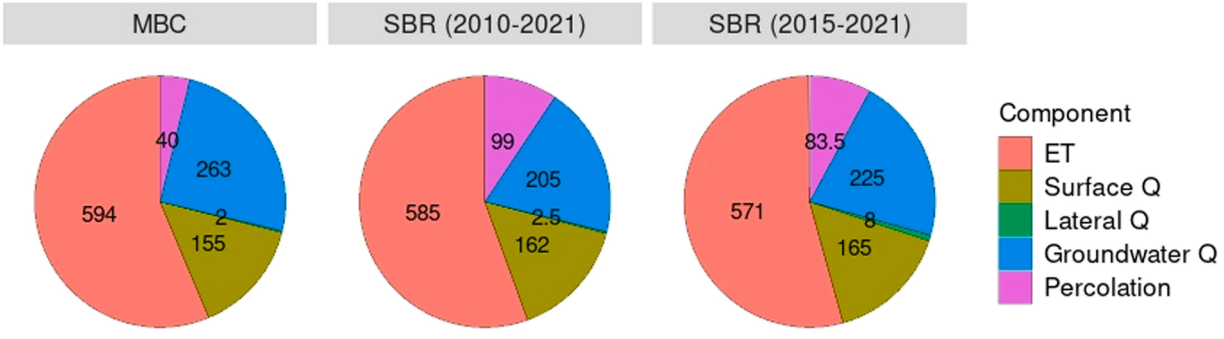

Fig. 4. Water balance components obtained from MBC, SBR (2010–2021), and SBR (2015–2021) (all units are in mm).

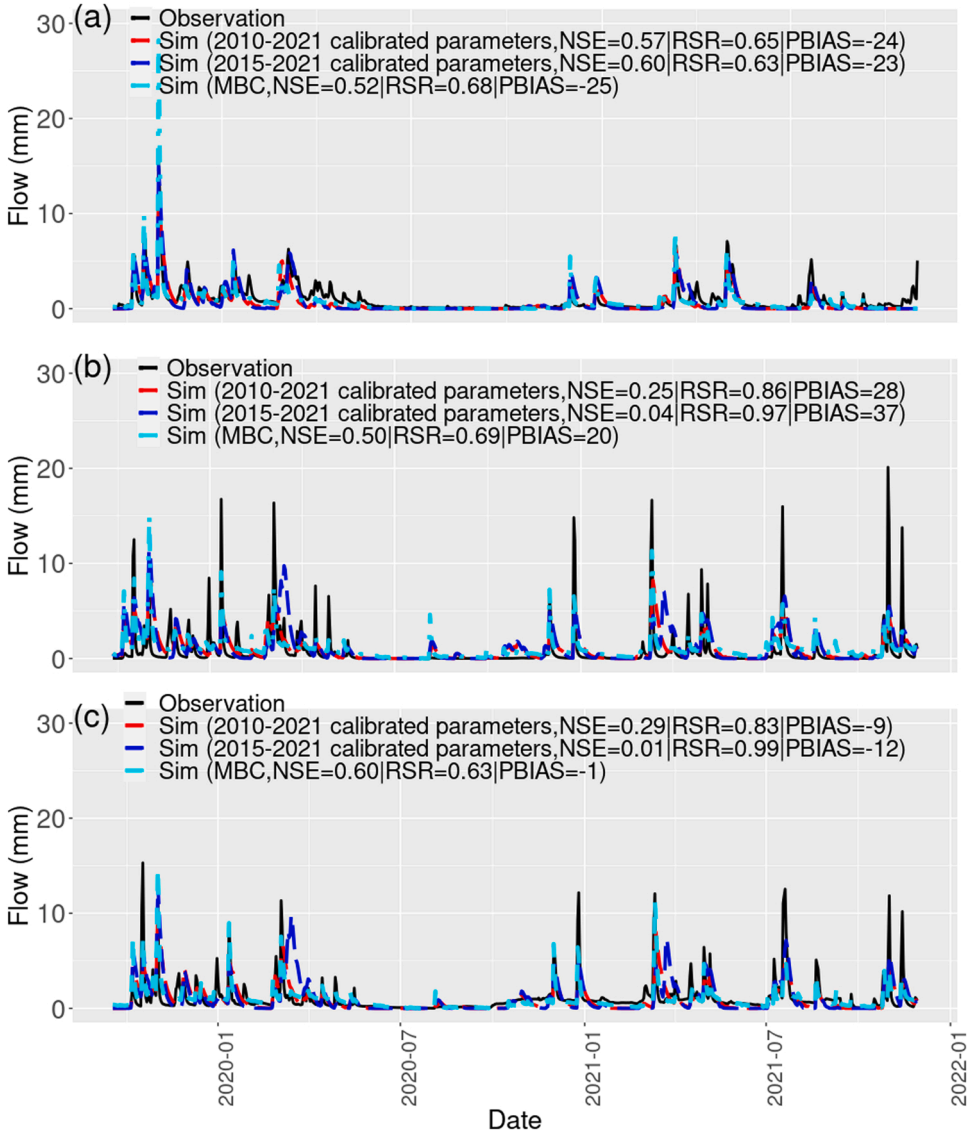

Fig. 5. Hydrographs of observed streamflow (black line) and simulated streamflow using SBR-2010–2021 (red dashed line) and SBR-2015–2021 (blue dashed line), and MBC (cyan dashed line) calibrated parameters for LOC-Monkton (a), WBDC (b), and EBDC (c). NSEs, RSRs, and PBIASes are evaluated on daily streamflow values.

water is available for evaporation in the soil layer (McNamara and Chandler, 2005; Woelber et al., 2018); this might also explain the greater ET values for MBC than SBR.

There are also some differences between ET parameter values between the two methods (Table 2). In MBC, the EPCO parameter, which controls the partitioning of the evaporative demand between the upper soil layer (near 0) and deeper soil layer (near 1) was lower (0.78), indicating that more plant water extraction occurs from the upper soil layer than in the SBR calibration (0.90). The ESCO value, which controls the evaporative demand from deeper soil layers is slightly lower in MBC than the SBR approaches, allowing the MBC model extracts moisture from deeper soil layers, allowing more ET. Indeed, ET using the MBC method was greater than the either SBR method (594 mm for MBC, 571 mm for SBR (2015–2021), and 585 mm for SBR (2010–2021) (Fig. 4). These values are in line with those of Church et al. (1995) and Shanley and Denner (1999) which showed the ET in the regions ranges between 500 and 600 mm or roughly 50 % of the water balance.

For parameters that influence groundwater (Table 2), the groundwater lag time (GW_DELAY) obtained from MBC (25.84) is greater than SBR (3.35–6.25), suggesting longer residence times for the MBC methods. The GW_DELAY is the time lag between the exit of water from the soil profile and its entry into the shallow aquifer. As the GW_DELAY increases, the shallow aquifer take longer to recharge. The greater GW_DELAY for the MBC method better represents the geomorphological characteristics of the watershed with the low permeability of clay soils, and is remarkably similar to the GW_DELAY of 25 days reported in TetraTech (2013) for the Little

Otter Creek watershed. The parameter that describes the threshold depth for return flow in shallow aquifers (GWQMN) is substantially greater for MBC (188) than for SBR (7.58–9.31), indicating considerably more water must be in the groundwater system for baseflow generation in MBC. Finally, the baseflow recession constant (ALPHA_BF) is higher for MBC (0.94) than SBR (0.52–0.91), indicating a more rapid response to recharge with very shallow groundwater levels. Combined the groundwater parameters resulted that greater groundwater contributions for MBC (263 mm) than for SBR (205 mm for 2010–2021 and 225 mm for 2015–2021). Deslandes et al. (2007) reported similar groundwater (271 mm) contributions using SWAT in the region.

3.3.2. *Comparison of flow generation between SBR and MBC*

The hydrographs and scatter plots of simulated and observed streamflow using calibrated parameters obtained from SBR-2010–2021 and SBR-2015–2021 and MBC are shown in Fig. 5 and Fig. 6. For the LOC-Monkton watershed using SBR for 2010–2021 and 2015–2021, peak flows, dry period, and water balance (as indicated by the proximity to the 1:1 line) of the simulation

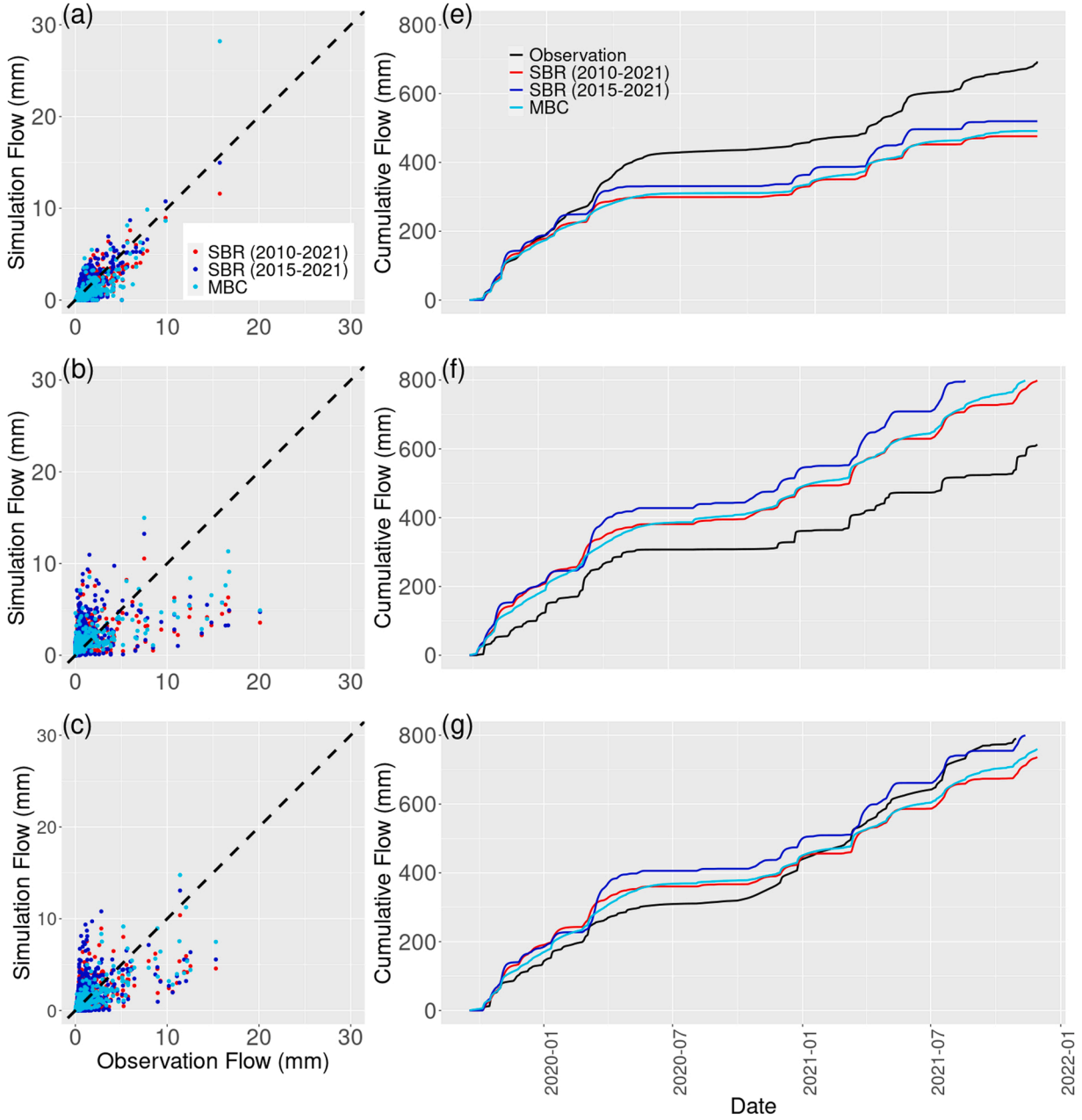

Fig. 6. Scatter plots and cumulative plots of observed (black lines) and simulated streamflow using the SBR-2010–2021 (red lines) and SBR-2015–2021 (blue lines), and MBC (cyan lines) calibrated parameters for LOC-Monkton (a and e), WBDC (b and f), and EBDC (c and g).

Table 3
The confidence intervals of NSE, RSR, and PBIAS obtained from the bootstrap test for model evaluation (95 % confidence level) and their performance rating as suggested by Moriasi et al. (2007).

Watershed	NSE (performance rating)			RSR (performance rating)			PBIAS (performance rating)		
	SBR (2010–2021)	SBR (2015–2021)	MBC	SBR (2010–2021)	SBR (2015–2021)	MBC	SBR (2010–2021)	SBR (2015–2021)	MBC
LOC-Monkton	0.44–0.75 (satisfactory)	0.41–0.79 (satisfactory)	0.40–0.66 (satisfactory)	0.56–0.76 (satisfactory)	0.46–0.65 (satisfactory)	0.36–0.71 (satisfactory)	-27 to − 16 (satisfactory)	-25 to − 15 (satisfactory)	-27 to − 17 (satisfactory)
WBDC	0.06–0.14 (unsatisfactory)	0.05–0.14 (unsatisfactory)	0.37–0.59 (satisfactory)	3.93–6.17 (unsatisfactory)	2.94–4.94 (unsatisfactory)	0.60–0.77 (satisfactory)	23–34 (unsatisfactory)	30–43 (unsatisfactory)	14–24 (satisfactory)
EBDC	0.06–0.17 (unsatisfactory)	0.03–0.18 (unsatisfactory)	0.43–0.68 (satisfactory)	2.35–3.37 (unsatisfactory)	1.87–2.74 (unsatisfactory)	0.54–0.70 (satisfactory)	-16 to − 5 (satisfactory)	20 to -8 (satisfactory)	-4 to − 1 (satisfactory)

approximately matched the observation (Fig. 5a and Fig. 6a). For the MBC method, the hydrograph of LOC-Monkton shows that although the magnitudes of some of the simulated storm events are moderately overestimated (Fig. 5a), the simulated results track the 1:1 line reasonably well (Fig. 6a). In both DCB watersheds, using SBR for 2010–2021 and 2015–2021, the peak flows were significantly underestimated (Figs. 5b and 5c). For both WBDC and EBDC, using MBC, the hydrographs show the models capture the timing relatively well, but they tend to underpredict storm events (Figs. 5b and 5c). The scatter plots (Figs. 6a, 6b, and 6c) show that, in all three watersheds, MBC results in tighter data points falling along the 1:1 line showing that this approach predicts hydrological mass balance better. Also, the results show that NSE using MBC for both DCB watersheds was substantially higher than those obtained using the SBR method.

Fig. 6 also shows cumulative observed and simulated flow for SBR and MBC for LOC-Monkton (Fig. 6e), WBDC (Fig. 6f), and EBDC (Fig. 6g). For LOC-Monkton and EBDC, all methods have similar cumulative flows that are also similar to the cumulative observed flow, although for LOC_Monkton slightly underestimated. For the WBDC watershed, the streamflow simulated using both methods followed similar patterns, although there was a tendency to overestimate flows.

3.4. Model evaluation and corroboration

The confidence intervals of the performance indicators (NSE, RSR, and PBIAS) with 95 % confidence level for SBR-2010–2021, SBR-2015–2021, and MBC methods and for each watershed are shown in Table 3, and indicate that the MBC method resulted in satisfactory model performance ratings for all NSE, RSR, and PBIAS in all three watersheds (Moriasi et al., 2007). SBR resulted in satisfactory model performance in LOC-Monkton, but similar to model calibration resulted in unsatisfactory model performance in WBDC and EBDC watersheds.

Table 4 shows soil parameter values, including average Depth (mm), AWC (mm/mm), and Ksat (mm/hr) obtained from SBR and MBC calibrations, corresponding values from the SSURGO database, and field measurements. As can be seen in Table 4, the MBC method provided parameter estimates that were more closely aligned with field measurements, whereas the average soil depth obtained from SBR is more closely aligned with SSURGO. For AWC, all estimated values obtained from calibration SBR and MBC are within the range of the field measurements. Calibrated Ksat values from MBC tended to most closely align with field measurements, while SBR Ksat values were better aligned with SSURGO estimates.

Although both approaches rely on the assumption of similarity between watersheds the MBC method results in more reasonable estimates of parameter values, and can be employed in areas without long term measurements. Indeed, the MBC method assumes the basins all have the same equations describing parameters, a very similar assumption to the similarity-based approach. However, the MBC approach ultimately provides the mean value for the basins included, rather than propagating one basin through the rest as in SBR. This not only allows the MBC to calibrate multiple basins with a much fewer observations, or shorter record, but also allows MBC to consider, in the calibration, a greater diversity of the regions' characteristics. Operationally, SBR also requires a neighboring donor watershed with a long period of recorded data which is difficult to find in a real-world application (Uereyen and Kuenzer, 2019).

4. Conclusions

This study introduced a new calibration method, MBC, for the calibration of watersheds with limited observed data. The MBC approach to parameter estimation of LDE is applicable in multiple neighboring basins with similar attributes, including land cover, soil type, mean annual precipitation, and temperature. The calibrated parameters and model performance were compared to the traditional SBR calibration method. To evaluate model parameters, we compared the soil storage parameters, including depth, AWC, and Ksat of MBC and SBR with the field measurements that showed the MBC methodology estimated the soil parameters with the closest values to the field measurements. The NSE values revealed that MBC outperformed SBR 2010–2021 and 2015–2021 for WBDC and EBDC. Streamflow simulations of both WBDC and EBDC models resulted in poor model performance for SBR 2010–2021 (0.25 and 0.29, respectively) and 2015–2021 (0.04 and 0.01, respectively). The MBC method enhanced the NSE of WBDC and EBDC to a satisfactory range (0.50 and 0.60, respectively). SBR methodology calibrates a donor watershed, while calibration of the MBC method extends over all LOCB and DCB watersheds, leading to better capture of watershed characteristics and estimation of model parameters. In addition, as previously mentioned, SBR and regionalization methods require at least one donor watershed; however, the vast majority of watersheds globally are unmonitored without any donor watersheds in their immediate vicinity. Thus, the MBC technique provides a framework for watershed modelers and hydrologists to quickly install streamflow gages in several neighboring watersheds

Table 4
Depth, AWC, and Ksat values from calibrated parameters of SBR (2010–2021), SBR (2015–2021), MBR, SSURGO, and field measurements.

Source	Soil depth (mm)	AWC (mm/mm)	Ksat (mm/h)
Calibration- SBR (2010–2021)	1081	0.25	29
Calibration- SBR (2015–2021)	927	0.24	27
Calibration-MBC	3017	0.26	7
SSURGO for LOCB	1280	0.18	48
SSURGO for DCB	960	0.15	10
Field measurements	> 3000 mm +	0.24	< 1*

* Ksat was quantified using the constant head permeameter and was so low that it was below the effective measurement range in many fields.

and use a short duration of measured streamflow data for their hydrological models and subsequent watershed management purposes. This study demonstrates that short periods of hydrological measurement from multiple locations in a basin can represent a system similarly to long-term measurements and that even short records taken at multiple locations significantly improve our hydrologic knowledge of a system as compared to relying on the similarity of nearby basins. This study used only three LDE watersheds, including more watersheds may improve the performance of the model because the information available to inform the model increases. The MBC technique improves the performance of hydrological models by incorporating more information using multiple basins during the calibration process. Future work could focus on assessing model uncertainty for both the SBR and MBC methods to determine whether incorporating more information as in the MBC method reduces model uncertainty. Finally, we should also note that the methodology has not been tested in other regions or under more diverse conditions, therefore, future work should focus on evaluating the method under new conditions and in other regions.

CRediT authorship contribution statement

Roja K. Garna: Conceptualization, Formal analysis, Investigation, Methodology, Visualization, Writing – original draft, Writing – review & editing. **Daniel R. Fuka:** Data curation, Conceptualization, Methodology, Resources, Software, Funding acquisition, Supervision, Validation, Writing – original draft, Writing – review & editing. **Joshua W. Faulkner:** Funding acquisition, Investigation, Writing – review & editing. **Amy S. Collick:** Writing – review & editing. **Zachary M. Easton:** Conceptualization, Funding acquisition, Methodology, Project administration, Writing – original draft, Writing – review & editing.

Declaration of Competing Interest

The authors declare that they have no known competing financial interests or personal relationships that could have appeared to influence the work reported in this paper.

Data Availability

Source code: Garna et al. (2022) https://doi.org/10.5281/zenodo.6609237.

Acknowledgments

We would like to acknowledge high-performance computing support provided by NCAR's Computational and Information Systems Laboratory (⟨https://doi.org/10.5065/D6RX99HX⟩) under Project no. UVIT0013, and from Virginia Tech's Advanced Research Computing Platform, funding support from the USDA under Project nos. 3072–13000-010-50S, NR193A750023C010 and 136396, DARPA award W911NF-18-1-0027 under subaward 97313118S and NSF under Project no. 1740704.

References

Ardia, D., 2009. DEoptim: differential evolution optimization in R. R package, version 1.3-3.
Arnold, J.G., Srinivasan, R., Muttiah, R.S., Williams, J.R., 1998. Large area hydrologic modeling and assessment Part i: model development. J. Am. Water Resour. Assoc. 34, 73–89. https://doi.org/10.1111/j.1752-1688.1998.tb05961.x.
Arnold, J.G., Kiniry, J.R., Srinivasan, R., Williams, J.R., Haney, E.B., Neitsch, S.L., 2013. SWAT 2012 Input/Output Documentation. Texas Water Resources Institute.
Arsenault, R., Brissette, F., Martel, J.-L., 2018. The hazards of split-sample validation in hydrological model calibration. J. Hydrol. 566, 346–362. https://doi.org/10.1016/j.jhydrol.2018.09.027.
Bao, Z., Zhang, J., Liu, J., Fu, G., Wang, G., He, R., Yan, X., Jin, J., Liu, H., 2012. Comparison of regionalization approaches based on regression and similarity for predictions in ungauged catchments under multiple hydro-climatic conditions. J. Hydrol. 466–467, 37–46. https://doi.org/10.1016/j.jhydrol.2012.07.048.
Beaudette, D.E., Skovlin, J., Roecker, S., Beaudette, M.D.E., 2021. Package "soilDB.".
Beven, K., 1993. Prophecy, reality and uncertainty in distributed hydrological modelling. Adv. Water Resour. 16, 41–51. https://doi.org/10.1016/0309-1708(93)90028-E.
Blöschl, G., Sivapalan, M., 1995. Scale issues in hydrological modelling: a review. Hydrol. Process. 9, 251–290. https://doi.org/10.1002/hyp.3360090305.
Buchanan, B., Auerbach, D.A., Knighton, J., Evensen, D., Fuka, D.R., Easton, Z., Wieczorek, M., Archibald, J.A., McWilliams, B., Walter, T., 2018. Estimating dominant runoff modes across the conterminous United States. Hydrol. Process. 32, 3881–3890. https://doi.org/10.1002/hyp.13296.
Canty, 2002. Resampling Methods in R: The Boot Package. The Newsletter of the R Project Volume.
Church, M.R., Bishop, G.D., Cassell, D.L., 1995. Maps of regional evapotranspiration and runoff/precipitation ratios in the northeast United States. J. Hydrol. 168, 283–298. https://doi.org/10.1016/0022-1694(94)02640-W.
Cibin, R., Sudheer, K.P., Chaubey, I., 2010. Sensitivity and identifiability of stream flow generation parameters of the SWAT model. Hydrol. Process. 24, 1133–1148. https://doi.org/10.1002/hyp.7568.
Collick, A.S., Fuka, D.R., Kleinman, P.J.A., Buda, A.R., Weld, J.L., White, M.J., Veith, T.L., Bryant, R.B., Bolster, C.H., Easton, Z.M., 2015. Predicting phosphorus dynamics in complex terrains using a variable source area hydrology model. Hydrol. Process. 29, 588–601. https://doi.org/10.1002/hyp.10178.
Daggupati, P., Pai, N., Ale, S., Douglas-Mankin, K.R., Zeckoski, R.W., Jeong, J., Parajuli, P.B., Saraswat, D., Youssef, M.A., 2015. A recommended calibration and validation strategy for hydrologic and water quality models. Trans. ASABE 58, 1705–1719. https://doi.org/10.13031/trans.58.10712.
Davis, T.W., Harke, M.J., Marcoval, M.A., Goleski, J., Orano-Dawson, C., Berry, D.L., Gobler, C.J., 2010. Effects of nitrogenous compounds and phosphorus on the growth of toxic and non-toxic strains of Microcystis during cyanobacterial blooms. Aquat. Microb. Ecol. 61, 149–162. https://doi.org/10.3354/ame01445.
Deshmukh, D., Ahmed, M.R., Dominic, J.A., Zaghloul, M.S., Gupta, A., Achari, G., Hassan, Q.K., 2022. Quantifying relations and similarities of the meteorological parameters among the weather stations in the Alberta Oil Sands region. PLoS One 17, e0261610. https://doi.org/10.1371/journal.pone.0261610.
Deslandes, J., Beaudin, I., Michaud, A., Bonn, F., Madramootoo, C.A., 2007. Influence of landscape and cropping system on phosphorus mobility within the pike river watershed of southwestern Quebec: model parameterization and validation. Can. Water Resour. J./Rev. Can. Ressour. Hydr. 32, 21–42. https://doi.org/10.4296/cwrj3201021.
Devia, G.K., Ganasri, B.P., Dwarakish, G.S., 2015. A review on hydrological models. Aquat. Procedia 4, 1001–1007. https://doi.org/10.1016/j.aqpro.2015.02.126.

Dewitz, J., 2021. National Land Cover Database (NLCD) 2019 Products [Dataset]. US Geological Survey, Sioux Falls, SD, USA.
Easton, Z.M., Fuka, D.R., Walter, M.T., Cowan, D.M., Schneiderman, E.M., Steenhuis, T.S., 2008. Re-Conceptualizing the Soil and Water Assessment Tool (SWAT) model to predict runoff from variable source areas. J. Hydrol. 348, 279–291.
Easton, Z.M., Walter, M.T., Fuka, D.R., White, E.D., Steenhuis, T.S., 2011. A simple concept for calibrating runoff thresholds in quasi-distributed variable source area watershed models. Hydrol. Process. 25, 3131–3143. https://doi.org/10.1002/hyp.8032.
Efron, B., 1992. Bootstrap methods: another look at the jackknife. In: Kotz, S., Johnson, N.L. (Eds.), Breakthroughs in Statistics: Methodology and Distribution. Springer New York, New York, NY, pp. 569–593 https://doi.org/10.1007/978-1-4612-4380-9_41.
Ehlers, L.B., Sonnenborg, T.O., Refsgaard, J.C., 2018. Observational and predictive uncertainties for multiple variables in a spatially distributed hydrological model. Hydrol. Process. https://doi.org/10.1002/hyp.13367.
Esmali, A., Golshan, M., Kavian, A., 2020. Investigating the performance of SWAT and IHACRES in simulation streamflow under different climatic regions in Iran. Atmósf. ER. https://doi.org/10.20937/atm.52740.
Farsadnia, F., Rostami Kamrood, M., Moghaddam Nia, A., Modarres, R., Bray, M.T., Han, D., Sadatinejad, J., 2014. Identification of homogeneous regions for regionalization of watersheds by two-level self-organizing feature maps. J. Hydrol. 509, 387–397. https://doi.org/10.1016/j.jhydrol.2013.11.050.
Feyereisen, G.W., Strickland, T.C., Bosch, D.D., Sullivan, D.G., 2007. Evaluation of SWAT manual calibration and input parameter sensitivity in the Little River watershed. Trans. ASABE 50, 843–855.
Fuka, D.R., Easton, Z.M., Brooks, E.S., Boll, J., Steenhuis, T.S., Walter, M.T., 2012. A simple process-based snowmelt routine to model spatially distributed snow depth and snowmelt in the SWAT Model1. J. Am. Water Resour. Assoc. 48, 1151–1161. https://doi.org/10.1111/j.1752-1688.2012.00680.x.
Fuka, D.R., Walter, M.T., MacAlister, C., Degaetano, A.T., Steenhuis, T.S., Easton, Z.M., 2014a. Using the climate forecast system reanalysis as weather input data for watershed models. Hydrol. Process. 28, 5613–5623. https://doi.org/10.1002/hyp.10073.
Fuka, D.R., Walter, M.T., MacAlister, C., Steenhuis, T.S., Easton, Z.M., 2014b. SWATmodel: a multi-operating system, multi-platform SWAT model package in R. J. Am. Water Resour. Assoc. 50, 1349–1353. https://doi.org/10.1111/jawr.12170.
Garna, R.K., Easton, Z.M., Faulkner, J.W., Collick, A.S., Fuka, D.R., 2022. Watershed model parameter estimation in low data environments. Zenodo. https://doi.org/10.5281/zenodo.6609237.
Gassman, P.W., Arnold, J.J., Srinivasan, R., Reyes, M., 2010. The worldwide use of the SWAT model: technological drivers, networking impacts, and simulation trends. In: 21st Century Watershed Technology: Improving Water Quality and Environment Conference Proceedings, 21–24 February 2010, Universidad EARTH, Costa Rica. American Society of Agricultural and Biological Engineers, p. 1.
Gassman, P.W., Balmer, C., Siemers, M., Srinivasan, R., 2014. The SWAT literature database: overview of database structure and key SWAT literature trends. In: SWAT 2014 Conference Pernambuco, Brazil: Conference Proceedings. Available: ⟨Http://swat.Tamu.edu/conferences/2014/⟩. (Accessed 27 June 2015).
Gupta, A., Govindaraju, R.S., 2019. Propagation of structural uncertainty in watershed hydrologic models. J. Hydrol. 575, 66–81. https://doi.org/10.1016/j.jhydrol.2019.05.026.
Her, Y., Chaubey, I., 2015. Impact of the numbers of observations and calibration parameters on equifinality, model performance, and output and parameter uncertainty. Hydrol. Process. 29, 4220–4237. https://doi.org/10.1002/hyp.10487.
Huang, J., Zhang, Y., Arhonditsis, G.B., Gao, J., Chen, Q., Peng, J., 2020. The magnitude and drivers of harmful algal blooms in China's lakes and reservoirs: a national-scale characterization. Water Res. 181, 115902 https://doi.org/10.1016/j.watres.2020.115902.
Hubbard, K.G., 1994. Spatial variability of daily weather variables in the high plains of the USA. Agric. For. Meteorol. 68, 29–41. https://doi.org/10.1016/0168-1923(94)90067-1.
Hui, J., Wu, Y., Zhao, F., Lei, X., Sun, P., Singh, S.K., Liao, W., Qiu, L., Li, J., 2020. Parameter optimization for uncertainty reduction and simulation improvement of hydrological modeling. Remote Sens. 12, 4069. https://doi.org/10.3390/rs12244069.
Jin, X., Xu, C.-Y., Zhang, Q., Singh, V.P., 2010. Parameter and modeling uncertainty simulated by GLUE and a formal Bayesian method for a conceptual hydrological model. J. Hydrol. 383, 147–155. https://doi.org/10.1016/j.jhydrol.2009.12.028.
Khorashadi Zadeh, F., Nossent, J., Sarrazin, F., Pianosi, F., van Griensven, A., Wagener, T., Bauwens, W., 2017. Comparison of variance-based and moment-independent global sensitivity analysis approaches by application to the SWAT model. Environ. Model. Softw. 91, 210–222. https://doi.org/10.1016/j.envsoft.2017.02.001.
LCBP, 2016. Lake Champlain Basin Program [WWW Document]. ⟨https://atlas.lcbp.org/⟩. (Accessed 25 December 2021).
Lebecherel, L., Andréassian, V., Perrin, C., 2016. On evaluating the robustness of spatial-proximity-based regionalization methods. J. Hydrol. 539, 196–203. https://doi.org/10.1016/j.jhydrol.2016.05.031.
Lee, H., McIntyre, N.R., Wheater, H.S., Young, A.R., 2006. Predicting runoff in ungauged UK catchments. Proc. Inst. Civ. Eng. - Water Manag. 159, 129–138. https://doi.org/10.1680/wama.2006.159.2.129.
Leta, O.T., Nossent, J., Velez, C., Shrestha, N.K., van Griensven, A., Bauwens, W., 2015. Assessment of the different sources of uncertainty in a SWAT model of the River Senne (Belgium). Environ. Model. Softw. 68, 129–146. https://doi.org/10.1016/j.envsoft.2015.02.010.
Lyon, S.W., Walter, M.T., Gérard-Marchant, P., Steenhuis, T.S., 2004. Using a topographic index to distribute variable source area runoff predicted with the SCS curve-number equation. Hydrol. Process. 18, 2757–2771. https://doi.org/10.1002/hyp.1494.
Masih, I., Uhlenbrook, S., Maskey, S., Ahmad, 2010. Regionalization of a conceptual rainfall–runoff model based on similarity of the flow duration curve: a case study from the semi-arid Karkheh basin, Iran. J. Hydrol. 391, 188–201. https://doi.org/10.1016/j.jhydrol.2010.07.018.
McNamara, J.P., Chandler, D., 2005. Soil moisture states, lateral flow, and streamflow generation in a semi-arid, snowmelt-driven catchment. Hydrological. ⟨https://onlinelibrary.wiley.com/doi/abs/10.1002/hyp.5869⟩.
Mengistu, A.G., van Rensburg, L.D., Woyessa, Y.E., 2019. Techniques for calibration and validation of SWAT model in data scarce arid and semi-arid catchments in South Africa. J. Hydrol.: Reg. Stud. 25, 100621 https://doi.org/10.1016/j.ejrh.2019.100621.
Menne, M.J., Durre, I., Vose, R.S., Gleason, B.E., Houston, T.G., 2012. An overview of the Global Historical Climatology Network-Daily database. J. Atmos. Ocean. Technol. 29, 897–910. https://doi.org/10.1175/JTECH-D-11-00103.1.
Merz, R., Blöschl, G., 2004. Regionalisation of catchment model parameters. J. Hydrol. 287, 95–123. https://doi.org/10.1016/j.jhydrol.2003.09.028.
Merz, R., Parajka, J., Blöschl, G., 2011. Time stability of catchment model parameters: Implications for climate impact analyses. Water Resour. Res. https://doi.org/10.1029/2010WR009505.
Mirza, M.M.Q., 2011. Climate change, flooding in South Asia and implications. Reg. Environ. Change 11, 95–107. https://doi.org/10.1007/s10113-010-0184-7.
Moebius-Clune, B.N., Moebius-Clune, D.J., Gugino, B.K., Idowu, O.J., Schindelbeck, R.R., Ristow, A.V., Van Es, H.M., Thies, J.E., Shayler, H.A., McBride, M.B., Wolfe, D.W., 2016. Comprehensive assessment of soil health. The Cornell Framework Manual, p. 3.
Moges, E., Demissie, Y., Larsen, L., Yassin, F., 2020. Review: sources of hydrological model uncertainties and advances in their analysis. Water 2021 (13), 28. https://doi.org/10.3390/w13010028.
Mohammed, S.A., Solomatine, D.P., Hrachowitz, M., 2021. Impact of dataset size on the signature-based calibration of a hydrological model. Water 2021 (13), 970. https://doi.org/10.3390/w13070970.
Moriasi, D.N., Arnold, J.G., Van Liew, M.W., Bingner, R.L., Harmel, R.D., Veith, T.L., 2007. Model evaluation guidelines for systematic quantification of accuracy in watershed simulations. Trans. ASABE 50, 885–900.
Mullen, K., Ardia, D., Gil, D.L., Windover, D., Cline, J., 2011. DEoptim: an R package for global optimization by differential evolution. J. Stat. Softw. 40, 1–26.
Nossent, J., Bauwens, W., 2012. Multi-variable sensitivity and identifiability analysis for a complex environmental model in view of integrated water quantity and water quality modeling. Water Sci. Technol. 65, 539–549. https://doi.org/10.2166/wst.2012.884.
Oeurng, C., Sauvage, S., Sánchez-Pérez, J.-M., 2011. Assessment of hydrology, sediment and particulate organic carbon yield in a large agricultural catchment using the SWAT model. J. Hydrol. 401, 145–153. https://doi.org/10.1016/j.jhydrol.2011.02.017.
Orth, R., Staudinger, M., Seneviratne, S.I., Seibert, J., Zappa, M., 2015. Does model performance improve with complexity? A case study with three hydrological models. J. Hydrol. 523, 147–159. https://doi.org/10.1016/j.jhydrol.2015.01.044.

Oudin, L., Andréassian, V., Perrin, C., Michel, C., Le Moine, N., 2008. Spatial proximity, physical similarity, regression and ungaged catchments: a comparison of regionalization approaches based on 913 French catchments. Water Resour. Res. 44. https://doi.org/10.1029/2007wr006240.
Parajka, J., Merz, R., Blöschl, G., 2005. A comparison of regionalisation methods for catchment model parameters. Hydrol. Earth Syst. Sci. 9, 157–171. https://doi.org/10.5194/hess-9-157-2005.
Peel, M.C., Chiew, F.H.S., Western, A.W., McMahon, T.A., 2000. Extension of Unimpaired Monthly Streamflow Data and Regionalisation of Parameter Values to Estimate Streamflow in Ungauged Catchments. Report to the National Land and Water Resources Audit.
Rafiei Emam, A., Kappas, M., Linh, N.H.K., Renchin, T., 2017. Hydrological modeling and runoff mitigation in an ungauged basin of central Vietnam using SWAT model. Hydrology 4, 16. https://doi.org/10.3390/hydrology4010016.
Randrianasolo, A., Ramos, M.H., Andréassian, V., 2011. Hydrological ensemble forecasting at ungauged basins: using neighbour catchments for model setup and updating. Adv. Geosci. 29, 1–11. https://doi.org/10.5194/adgeo-29-1-2011.
Renard, B., Kavetski, D., Kuczera, G., Thyer, M., Franks, S.W., 2010. Understanding predictive uncertainty in hydrologic modeling: the challenge of identifying input and structural errors. Water Resour. Res. 46. https://doi.org/10.1029/2009wr008328.
Ruggiero, R., Ross, D., Faulkner, J.W., 2022. Tile drainage flow partitioning and phosphorus export in Vermont USA. Collect. FAO Agric. 12, 167. https://doi.org/10.3390/agriculture12020167.
Saltelli, A., 2004. Global sensitivity analysis: an introduction. In: Proc. 4th International Conference on Sensitivity Analysis of Model Output (SAMO'04). Citeseer, p. 43.
Samuel, J., Coulibaly, P., Metcalfe, R.A., 2011. Estimation of continuous streamflow in Ontario ungauged basins: comparison of regionalization methods. J. Hydrol. Eng. 16, 447–459. https://doi.org/10.1061/(asce)he.1943-5584.0000338.
Schiermeier, Q., 2011. Increased flood risk linked to global warming. Nature. https://doi.org/10.1038/470316a.
Seibert, J., Staudinger, M., van Meerveld, H.J. (ilja), 2019. Validation and over-parameterization—experiences from hydrological modeling. In: Beisbart, C., Saam, N. J. (Eds.), Computer Simulation Validation: Fundamental Concepts, Methodological Frameworks, and Philosophical Perspectives. Springer International Publishing, Cham, pp. 811–834. https://doi.org/10.1007/978-3-319-70766-2_33.
Sellami, H., La Jeunesse, I., Benabdallah, S., Baghdadi, N., Vanclooster, M., 2014. Uncertainty analysis in model parameters regionalization: a case study involving the SWAT model in Mediterranean catchments (Southern France). Hydrol. Earth Syst. Sci. 18, 2393–2413. https://doi.org/10.5194/hess-18-2393-2014.
Setegn, S.G., Srinivasan, R., Melesse, A.M., Dargahi, B., 2009. SWAT model application and prediction uncertainty analysis in the Lake Tana Basin, Ethiopia. Hydrol. Process. https://doi.org/10.1002/hyp.7457.
Shanley, J.B., Denner, J.C., 1999. The hydrology of the Lake Champlain basin. In: Lake Champlain in Transition: From Research Toward Restoration, Water Science and Application. American Geophysical Union, Washington, D. C, pp. 41–66. https://doi.org/10.1029/ws001p0041.
Shi, P., Chen, C., Srinivasan, R., Zhang, X., Cai, T., Fang, X., Qu, S., Chen, X., Li, Q., 2011. Evaluating the SWAT model for hydrological modeling in the Xixian watershed and a comparison with the XAJ model. Water Resour. Manag. 25, 2595–2612. https://doi.org/10.1007/s11269-011-9828-8.
Singh, S.K., Bárdossy, A., 2012. Calibration of hydrological models on hydrologically unusual events. Adv. Water Resour. 38, 81–91. https://doi.org/10.1016/j.advwatres.2011.12.006.
Singh, V.P., Frevert, D.K., 2002. Mathematical Models of Large Watershed Hydrology. Water Resources Publication.
Sivapalan, M., Takeuchi, K., Franks, S.W., Gupta, V.K., Karambiri, H., Lakshmi, V., Liang, X., McDonnell, J.J., Mendiondo, E.M., O'connell, P.E., Oki, T., Pomeroy, J. W., Schertzer, D., Uhlenbrook, S., Zehe, E., 2003. IAHS decade on predictions in ungauged basins (PUB), 2003–2012: shaping an exciting future for the hydrological sciences. Hydrol. Sci. J. 48, 857–880. https://doi.org/10.1623/hysj.48.6.857.51421.
Sorooshian, S., Hsu, K.-L., Coppola, E., Tomassetti, B., Verdecchia, M., Visconti, G., 2008. Hydrological Modelling and the Water Cycle: Coupling the Atmospheric and Hydrological Models. Springer Science & Business Media.
Stewart, D.P., Macclintock, P., 1969. The Surficial Geology and Pleistocene History of Vermont. Vermont Geological Survey and Department of Water Resources.
Tegegne, G., Kim, Y.-O., 2018. Modelling ungauged catchments using the catchment runoff response similarity. J. Hydrol. 564, 452–466. https://doi.org/10.1016/j.jhydrol.2018.07.042.
TetraTech, 2013. Lake Champlain Basin SWAT Model Configuration, Calibration and Validation. Prepared for EPA Region.
Trenberth, K.E., 2005. The impact of climate change and variability on heavy precipitation, floods, and droughts. Encycl. Hydrol. Sci. 17. https://doi.org/10.1002/0470848944.hsa211.
Trenberth, K.E., 2009. Precipitation in a changing climate-more floods and droughts in the future. Gewex N. 19 (May 2009), 8–10.
Troy, A., Wang, D., Capen, D., O'Neil-Dunne, J., MacFaden, S., 2007. Updating the Lake Champlain Basin Land Use Data to Improve Prediction of Phosphorus Loading. Report to the Lake Champlain Basin Program. LCBP Technical Report, Grand Isle, Vermont.
Twombly, C.R., Faulkner, J.W., Collick, A.S., Easton, Z.M., 2021. Identification of phosphorus index improvements through model comparisons across topographic regions in a small agricultural watershed in Vermont (USA). Soil Sci. Soc. Am. J. 85, 1226–1241. https://doi.org/10.1002/saj2.20254.
U.S. Geological Survey, 2022. National Water Information System data available on the World Wide Web (USGS Water Data for the Nation) [WWW Document]. ⟨https://doi.org/10.5066/F7P55KJN⟩.
U.S. Geological Survey, 2021a. USGS 04282650 LITTLE OTTER CREEK AT FERRISBURG, VT, in USGS water data for the Nation: U.S. Geological Survey National Water Information System database [WWW Document]. ⟨https://waterdata.usgs.gov/nwis/uv/?site_no=04282650⟩. (Accessed 28 December 2021).
U.S. Geological Survey, 2021b. USGS 04282629 LITTLE OTTER CK AT MONKTON RD, NR FERRISBURGH, VT, in USGS water data for the Nation: U.S. Geological Survey National Water Information System database [WWW Document]. ⟨https://waterdata.usgs.gov/nwis/uv/?site_no=04282629⟩. (Accessed 28 December 2021).
U.S. Geological Survey, 2021c. USGS 04282586 WEST BR DEAD CREEK NEAR ADDISON, VT, in USGS water data for the Nation: U.S. Geological Survey National Water Information System database [WWW Document]. ⟨https://waterdata.usgs.gov/nwis/uv/?site_no=04282586⟩. (Accessed 26 December 2021).
U.S. Geological Survey, 2021d. USGS 04282581 EAST BR DEAD CREEK NEAR BRIDPORT, VT, in USGS water data for the Nation: U.S. Geological Survey National Water Information System database [WWW Document]. ⟨https://waterdata.usgs.gov/nwis/uv/?site_no=04282581⟩. (Accessed 26 December 2021).
Uereyen, S., Kuenzer, C., 2019. A review of Earth observation-based analyses for major river basins. Remote Sens. 11, 2951. https://doi.org/10.3390/rs11242951.
USDA NRCS, 2019. USDA announces water quality study in Vermont's Lake Champlain Basin [WWW Document]. ⟨https://www.nrcs.usda.gov/wps/portal/nrcs/detail/national/newsroom/releases/?cid=NRCSEPRD1495437/⟩. (Accessed 11 June 2020).
van Griensven, A., Meixner, T., Grunwald, S., Bishop, T., Diluzio, M., Srinivasan, R., 2006. A global sensitivity analysis tool for the parameters of multi-variable catchment models. J. Hydrol. 324, 10–23. https://doi.org/10.1016/j.jhydrol.2005.09.008.
Vandewiele, G.L., Elias, A., 1995. Monthly water balance of ungauged catchments obtained by geographical regionalization. J. Hydrol. 170, 277–291. https://doi.org/10.1016/0022-1694(95)02681-E.
Veith, T.L., Van Liew, M.W., Bosch, D.D., Arnold, J.G., 2010. Parameter sensitivity and uncertainty in SWAT: a comparison across five USDA-ARS watersheds. Trans. ASABE 53, 1477–1486.
Vemuri, V., Dracup, J.A., Erdmann, R.C., Vemuri, N., 1969. Sensitivity analysis method of system identification and its potential in hydrologic research. Water Resour. Res. 5, 341–349. https://doi.org/10.1029/wr005i002p00341.
Wagena, M.B., Easton, Z.M., 2018. Agricultural conservation practices can help mitigate the impact of climate change. Sci. Total Environ. 635, 132–143. https://doi.org/10.1016/j.scitotenv.2018.04.110.
Wagena, M.B., Sommerlot, A., Abiy, A.Z., Collick, A.S., Langan, S., Fuka, D.R., Easton, Z.M., 2016. Climate change in the Blue Nile Basin Ethiopia: implications for water resources and sediment transport. Clim. Change 139, 229–243. https://doi.org/10.1007/s10584-016-1785-z.
Wagena, M.B., Bhatt, G., Buell, E., Sommerlot, A.R., Fuka, D.R., Easton, Z.M., 2019. Quantifying model uncertainty using Bayesian multi-model ensembles. Environ. Model. Softw. 117, 89–99. https://doi.org/10.1016/j.envsoft.2019.03.013.
Wambura, F.J., Dietrich, O., Lischeid, G., 2018. Improving a distributed hydrological model using evapotranspiration-related boundary conditions as additional constraints in a data-scarce river basin. Hydrol. Process. 32, 759–775. https://doi.org/10.1002/hyp.11453.

Web Soil Survey, 2019. Natural Resources Conservation Service, United States Department of Agriculture [WWW Document]. ⟨http://websoilsurvey.sc.egov.usda.gov/⟩. (Accessed 5 January 2021).

Woelber, B., Maneta, M.P., Harper, J., Jencso, K.G., Gardner, W.P., Wilcox, A.C., López-Moreno, I., 2018. The influence of diurnal snowmelt and transpiration on hillslope throughflow and stream response. Hydrol. Earth Syst. Sci. 22, 4295–4310. https://doi.org/10.5194/hess-22-4295-2018.

Yadav, M., Wagener, T., Gupta, H., 2007. Regionalization of constraints on expected watershed response behavior for improved predictions in ungauged basins. Adv. Water Resour. 30, 1756–1774. https://doi.org/10.1016/j.advwatres.2007.01.005.